JOURNAL OF SOLID STATE CHEMISTRY 53, 120–129 (1984)

Systematics of the Pyrochlore Structure Type, Ideal $A_2B_2X_6Y$

BRYAN C. CHAKOUMAKOS*

Department of Geological Sciences, Virginia Polytechnic Institute and State University, Blacksburg, Virginia 24061

Received October 14, 1983; in revised form January 20, 1984

The geometry of the ideal pyrochlore struture type ($^8A_2{}^6B_2{}^4X_6{}^4Y$, $Fd3m$) has been examined using a data base of 440 synthetic samples. Mean ionic radii of the cubic and octahedral cations together account for 95% of the variation in the cell edge. Nonempirical expressions for calculating the cell edge are also derived, using that the interatomic distances are functions of the cell edge and a single positional parameter, x, of the X anion. This alternative method is equally successful for calculating the cell edge, and additionally provides for the calculation of x. Comparison of calculated x values with 27 experimentally measured values indicates that the stoichiometry, x values, or bond length predicting radii are in error for 20% of these pyrochlores. For 21 observed x values judged to be most accurate, the calculated anion coordinates are within 0.009. In addition, calculated x values are given for 400 pyrochlores for which no values have been previously determined.

Introduction

Materials of the pyrochlore structure type, with their wide range in chemistry, exhibit a variety of potentially useful properties, which include catalysis (*1*), ferroelectricity (*2*), ferromagnetism (*3*), luminescence (*4*), and ionic conductivity (*5*). As the pyrochlore-related phase, zirconolite, is important in proposed crystalline nuclear waste forms (*6*), pyrochlore phases themselves may have a similar potential. The pyrochlore structure type is also represented in a wide range of natural occurrences by the mineral groups pyrochlore, microlite, betafite, and stibiconite (*7*). A recent review of the crystal chemistry and applications of oxide pyrochlores is given by Subramanian *et al.* (*8*).

The structure is cubic, $Fd3m$, $Z = 8$, and is commonly described as a fluorite structure derivative (*9*). This description is achieved by removing $\frac{1}{8}$ of the anions in an ordered fashion, such that one-half of the cubic polyhedra are missing two opposed vertices. Alternative descriptions of the structure type are reviewed elsewhere (*8*). The structural formula for ideal pyrochlore is $^8A_2{}^6B_2{}^4X_6{}^4Y$, where A and B are metal cations and X and Y are anions. The coordinations of the ions in the ideal case are AX_6Y_2, BX_6, XA_2B_2, and YA_4. By removing combinations of A and Y ions, a variety of defect structures (e.g., $^6A_2{}^6B_2{}^4X_6$, $^6A^6B_2{}^3X_6$) can be produced which are known to occur with the general formula $A_{1-2}B_2X_6Y_{0-1}$. Another structural variant, $\square{}^6B_2{}^3X_6{}^6M$, referred to as "inverse" pyrochlore by Barker *et al.* (*10*), has the same B_2X_6 framework, but with the A cation positions vacant and the Y anions replaced by large monovalent cations.

* Present address: Department of Geology, University of New Mexico, Albuquerque, N. Mex. 87131.

0022-4596/84 $3.00

TABLE I

INTERATOMIC DISTANCES AS A FUNCTION OF THE UNIT CELL EDGE a AND THE X ANION POSITIONAL PARAMETER x FOR $A_2B_2X_6Y$ PYROCHLORE, WHERE A AND B ARE THE CUBIC AND OCTAHEDRAL CATIONS RESPECTIVELY, AND X AND Y ARE ANIONS

Atom pair	Distance	Comments
$A \ldots A$	$a\sqrt{2}/4$	Cub–cub cation separation
$A \ldots B$	$a\sqrt{2}/4$	Cub–oct cation separation
$B \ldots B$	$a\sqrt{2}/4$	Oct–oct cation separation
A–X	$a(x^2 - \frac{1}{2}x + \frac{3}{32})^{0.5}$	Cub bond (equatorial)
A–Y	$a\sqrt{3}/8$	Cub bond (axial)
B–X	$a(x^2 - x + \frac{9}{32})^{0.5}$	Oct bond
$X \ldots Y$	$a(x - \frac{1}{8})$	Shared cub-cub edge
$X \ldots X$	$a(2x^2 - \frac{3}{2}x + \frac{11}{32})^{0.5}$	Shared cub-oct edge
$X \ldots X$	$a\sqrt{2}(\frac{5}{8} - x)$	Unshared oct edge

Note. The x values correspond to the cell origin at the A cation on the 16c positions. For the alternative origin choices at B or Y, replace x by $(\frac{3}{4} - x)$ and $(x - \frac{1}{8})$, respectively.

In this paper the geometry of the ideal pyrochlore structure type has been examined using a data base of 440 synthetic samples. The equations and diagrams presented allow for the rapid interpretation of the internal consistency of published data, and the prediction of the structural parameters for hypothetical or partially studied pyrochlores.

Geometry of the Pyrochlore Structure Type

All the atoms in the pyrochlore unit cell occupy special positions in the space group $Fd3m$ (No. 227, origin at 16c, $\bar{3}m$); A—16c, B—16d, X—48f, and Y—8a. The atomic arrangement is completely specified, except for the x coordinate of the 48f positions. The principal interatomic distances can be expressed as functions of the x coordinate and the cell edge a (Table I), and are graphically portrayed for the ranges of x and a values of interest in Fig. 1. Varying the x coordinate changes the shapes of the A- and B-site polyhedra. For $x = 0.3750$ the X anions are arranged as in the anion-deficient fluorite derivative. At this value of x the A- and B-site polyhedra are regular cubes and trigonally flattened octahedra, respectively. When the x coordinate increases to 0.4375 the B-site becomes a regular octahedron, and the cubic A-site distorts into a trigonal scalenohedron. With further increase in x the B-site elongates along a threefold and the A-site becomes a hexagonal bipyramid.

Using the expressions in Table I, the ratio of the mean cubic to octahedral bond lengths, R, is defined as

$$R = \frac{\langle A\text{–}XY\rangle}{B\text{–}X} = \frac{0.75(x^2 - 0.5x + \frac{3}{32})^{0.5} + 0.25\sqrt{3}/8}{(x^2 - x + \frac{9}{32})^{0.5}} \quad [1]$$

where $\langle A\text{–}XY\rangle = 0.75(A\text{–}X) + 0.25(A\text{–}Y)$. To solve Eq. [1] in terms of R, a best-fit polynomial has been determined by the method of least squares. The resulting polynomial

$$x = -0.751846 + 3.63005R - 5.03230R^2 + 3.57083R^3 - 1.09316R^4 + 0.051435R^6 \quad [2]$$

gives the value of x with a precision of 0.00009 for the range 0.35 to 0.50.

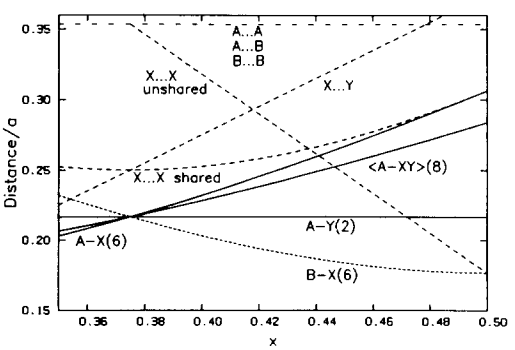

FIG. 1. Principal interatomic distances in $A_2B_2X_6Y$ pyrochlore $Fd3m$ (origin at 16c) given as *distance/a* ratios, which are functions of the X anion positional parameter x. Labels correspond to those in Table I, and appear directly below each curve. The numbers in parentheses are the multiplicities of the bonds (after Hoekstra and Siegel (*11*)).

By strict adherence to a "hard sphere" model, the A cation size would be determined by the short axial A–Y bond distances (for $x > 0.3750$). However, reasonable results are obtained only by using the weighted average cubic bond length, i.e., relative to the sums of bond length predicting radii (*12*), the observed A–Y distances are shorter and the observed A–X distances are longer.

Another method for calculating the anion positional parameter of an oxide pyrochlore based on a geometrical description was devised by Nikiforov (*13*). His method consisted of two inequalities, given here for the origin choice A at 16c,

$$\tfrac{1}{8} + 2rX/a \leq x \leq \tfrac{5}{8} - \sqrt{2}rX/a \quad [3]$$

$$\tfrac{1}{2} - [(rB + rX)^2/a^2 - \tfrac{1}{32}]^{0.5} \leq x \leq \tfrac{1}{2} - \tfrac{1}{8}[3(rB + rX)^2/(rA + rY)^2 - 2]^{0.5} \quad [4]$$

where rA, rB, rX, and rY are the radii of the A, B, X, and Y ions, respectively. Equation [3] is derived from the expressions in Table I by assuming that the $X \ldots X$ unshared octahedral edge and the $X \ldots Y$ shared cube–cube edge are both greater than or equal to the sum of two oxide radii. The assumptions which led to Eq. [4] are that B–$X \leq rB + rX$, A–$Y \leq rA + rY$, and $(rA + rY) - (A$–$Y) > (rB + rX) - (B$–$X)$. By solving Eqs. [3] and [4] together, a range of x values can be calculated for an oxide pyrochlore whose cell edge has been measured. Shortcomings of this method are that (1) a range for x is obtained rather than a single value, (2) the right side of Eq. [4] cannot be solved when $(rB + rX)/(rA + rY) > \sqrt{2/3}$, (3) Eq. [4] requires a measurement of the cell edge, (4) the assumptions leading to Eq. [4] are to some extent empirical, and (5) pyrochlores with the Y anion other than O^{2-} are not considered.

McCauley (*14*) has computed the anion positional parameters for a large number of $A^{3+}B^{4+}$ pyrochlores using the relationships developed by Nikiforov. For those pyrochlores for which shortcoming (2) above did not prohibit the calculation, McCauley reported exact x values by averaging the extremes of the range of x calculated by the inequalities. He found that the difference between calculated and measured x values for 11 pyrochlores was 1.5%, however no statistical analysis was reported. The variations of the calculated x values with cation composition did agree with the experimental results summarized by Barker *et al.* (*15*), that increasing the radius of the A^{3+} cation in a series of constant B^{4+} increases the value of x, and that increasing the radius of the B^{4+} cation in a series of constant A^{3+} decreases the value of x.

Statistical Analysis

Table II[1] is a listing of 440 synthetic $A_2B_2O_6Y$ pyrochlores for which compositions and cell edges have been reported. The list is arranged alphabetically, first according to the elemental symbol of the B cations and then by the elemental symbol of the A cations. Table II is not necessarily a complete nor critical compilation of all the reported data; however, it does include a large variety of compositions. For the oxyfluoride and oxysulfide pyrochlores, only those compositions with no more than one fluorine or sulfur substituting for oxygen are included. For convenience in those cases, the F or S is placed at the Y site, despite that for the oxyfluoride pyrochlores no experimental confirmation of this anion

[1] See NAPS document No. 04165 for 10 pages of supplementary material. Order from ASIS/NAPS, Microfiche Publications, P.O. Box 3513, Grand Central Station, New York, NY 10163. Remit in advance $4.00 for microfiche copy or for photocopy, $7.75 up to 20 pages plus $.30 for each additional page. All orders must be prepaid. Institutions and organizations may order by purchase order. However, there is a billing and handling charge for this service of $15. Foreign orders add $4.50 for postage and handling, for the first 20 pages, and $1.00 for additional 10 pages of material. Remit $1.50 for postage of any microfiche orders.

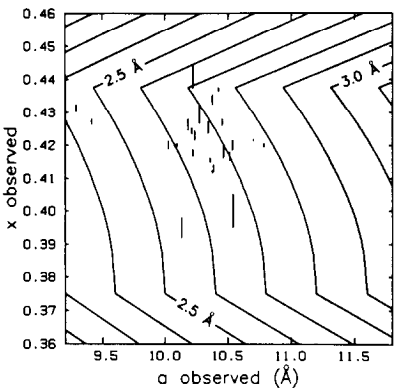

FIG. 2. X anion positional parameter x versus the cell edge a observed for $A_2B_2X_6Y$ pyrochlores are shown as vertical lines, where the line length indicates the reported error in x. The reported errors in a are all smaller than the linewidth, so horizontal bars do not appear. The contour lines display how the minimum anion separation (X . . . X shared, X . . . X unshared, or X . . . Y) varies as a function x and a. The contour interval is 0.1 Å (after Ewing and Chakoumakos (*16*)).

distribution has been made. Measurements of the positional parameter, x, of the X anion have been reported for 27 of the pyrochlores tabulated.

These 27 reported values are shown on a contour map (Fig. 2) of the nearest-neighbor anion separation, plotted as a function of the cell edge a and the positional parameter x. The pattern of contours is determined by the minimum values of the X . . . X shared, X . . . X unshared, and X . . . Y curves in Fig. 1. For each cell edge, the nearest-neighbor anion separation is maximum at $x = 0.4375$, and this separation closely corresponds to the sum of two oxide and/or fluoride radii. The interval $x = 0.3750$–0.4375 defines a band of anion separations that are close to the maximum value. Outside this range, the anion separation shortens much more rapidly as x changes. The pyrochlores, whose x values have been experimentally measured, cluster along the band of maximum anion separation. The average x value, 0.422 (±0.010), is smaller than the maximum anion separation at 0.4375; however, the average is close to 0.41789, which occurs when the shared cub–oct edge (X . . . X shared) equals the shared cub–cub edge (X . . . Y). Madelung constants, which have been computed for the most common combinations of ionic species forming pyrochlore compounds (*10, 15, 17*), suggest that the x coordinate should be somewhat greater than 0.4375 to maximize the electrostatic energy. This suggested to Barker *et al.* (*10*) that the inclusion of the repulsion energy into the enthalpy of formation expression is critical in determining the relative stability of pyrochlore compounds. Figure 2 illustrates qualitatively the effect of anion–anion repulsions as x is varied, i.e., repulsive energies would be greatest for the smallest anion separations.

For those pyrochlores in Table II for which the cation valence states could be assigned, mean ionic radii were obtained for the cubic cations, rA, and the octahedral cations, rB, using the ionic radii of Shannon (*12*). These values were included in a regression analysis against the cell edge for the full data set and also for three subgroups of different average valence combinations, $A^{3+}B^{4+}$, $A^{2+}B^{5+}$ and others. The model containing both radii was significant in each case, and the least-squares planes obtained (Table III) account for 95.4% of the variation in cell edge for the full data, 96.2% for $A^{3+}B^{4+}$, 90.7% for $A^{2+}B^{5+}$, and 96.8% for others. The mean ionic radii were also individually included in regressions against the cell edge to establish if either rA or rB accounts for the cell edge variation more significantly. For the full data set, rA and rB individually account for 67.0 and 70.5% of the variation in the cell edge, respectively. This result supports the descriptions of the pyrochlore structure as an interpenetration of two beta-cristobalite sublattices ($\square B_2X_6$ and YA_2) (*18*), rather than as a relatively stable B_2X_6 framework with the A and Y ions filling interstices.

TABLE III

LINEAR REGRESSION ANALYSES

Dependent variable	Independent variable(s)	Data group	Sample size	Least squares estimate[a] Slopes		Intercept	σ^2	r^2 (%)
a obs.	rA, rB	All	437	1.654(34) (0.0001)	3.211(62) (0.0001)	6.492(40) (0.0001)	0.057	95.4
a obs.	rA, rB	$A^{3+}B^{4+}$	248	1.914(54) (0.0001)	2.910(58) (0.0001)	6.422(53) (0.0001)	0.047	96.2
a obs.	rA, rB	$A^{2+}B^{5+}$	34	1.22(15) (0.0001)	3.99(32) (0.0001)	6.52(22) (0.0001)	0.064	90.7
a obs.	rA, rB	Other	155	1.473(57) (0.0001)	4.24(14) (0.0001)	6.013(68) (0.0001)	0.052	96.8
a obs.	a calc.	All	437	0.989(12) (0.0001)		0.08(12) (0.51)	0.065	94.3
a obs.	a calc.	$A^{3+}B^{4+}$	248	1.033(14) (0.0001)		−0.35(14) (0.016)	0.047	95.6
a obs.	a calc.	$A^{2+}B^{5+}$	34	0.930(61) (0.0001)		0.67(64) (0.30)	0.071	87.9
a obs.	a calc.	Other	155	1.047(21) (0.0001)		−0.55(22) (0.012)	0.069	94.3
x obs.	x calc.	All	27	1.01(24) (0.0003)		0.00(10) (0.99)	0.008	41.4
x obs.	x calc.	Accurate	21	0.677(89) (0.0001)		0.139(37) (0.0014)	0.003	75.3
x obs.	x calc. Nikiforov	Accurate	21	0.18(30) (0.55)		0.34(13) (0.015)	0.005	1.9

[a] Estimated standard error and probability significance of the t statistic are given in parentheses to the right and below respectively, for each least-squares estimated parameter.

[b] Estimated standard deviation of the residuals from the regression.

The analysis thus far consists of empirical relationships, which have value for prediction of the cell edge, but are inconvenient in that the equations require constant updating as new and improved data become available. The following alternative approach is based upon the geometry of the pyrochlore cell and the constancy of bond lengths given that they have the same chemical environment.

The geometrical description of the unit cell in the previous section led to Eq. [2], which gives the X anion positional parameter as a function of the ratio of the mean cubic to octahedral bond lengths, $\langle A\text{–}XY\rangle/(B\text{–}X)$. The values of rA and rB of Table II along with $r(^4O^{2-}) = 1.38$, $r(^4F^-) = 1.31$, and $r(^4S^{2-}) = 1.68$ Å[2] were used to obtain $\langle A\text{–}XY\rangle$ and $(B\text{–}X)$; then values of x were calculated with Eq. [2]. Figure 3 is a comparison between the 27 observed x values and those calculated by Eq. [2]. Linear regression analysis of the observed x against the calculated x yields a poor correlation (Table III). Before the quality of the measured x values can be judged by comparison with the calculated values, a set of bond length predicting radii consistent for the pyrochlore group must be employed. If the

[2] The $^4S^{2-}$ radius, not reported by (*12*), was estimated.

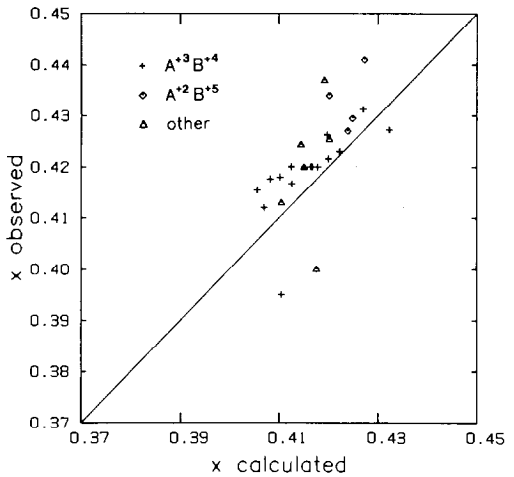

FIG. 3. Observed X anion positional parameters, x, are compared with those calculated for $A_2B_2X_6Y$ pyrochlores. The solid line is the one-to-one relationship.

radii sums are not accurate estimates of $\langle A\text{–}XY\rangle$ and $(B\text{–}X)$, then the calculated x value will be wrong. The six most discrepant points in Fig. 3 include pyrochlores in which the A-site has Cd^{2+} ($Cd_2Nb_2O_7$, $Cd_2Re_2O_7$, $Cd_2Ta_2O_7$, and $Bi_{0.4}Cd_{1.6}Ta_{1.87}Cd_{0.13}O_7$). The other two are $Bi_{1.5}Zn_{0.5}Ta_{1.5}Zn_{0.5}O_7$ and $Tl_2Pt_2O_7$. For these six compositions the radii sums do not match the observed $\langle A\text{–}XY\rangle$ and $(B\text{–}X)$ distances determined by the measured x values. Errors in the stoichiometry, x value, or bond length predicting radii, could be responsible. When these six points are excluded, the correlation between the measured and calculated x values improves to $r^2 = 0.75$ (Table III); the calculated values deviate from the observed by at most 0.009. Examination of Fig. 3 reveals that even for the "accurate 21" x value measurements the calculated x values appear to be systematically low by about 0.005. A comparison of the observed mean bond lengths with their radii sums reveals the source of the systematic error. The mean $\langle A\text{–}XY\rangle$ distances are shorter on average by 0.021 Å than the observed distances, and B–X is greater by 0.019 Å than the observed. Consequently, R is systematically smaller, which results in the calculated x values being slightly small. Further assessment of the quality of the x values must be deferred until more structure refinements and better bond length predicting radii become available.

Before continuing, Nikiforov's method for calculating the anion positional parameter is tested to compare it with the new method discussed above. For the "accurate 21" subset of data mentioned previously, Nikiforov's inequalities have been solved to give single values of x in the same manner as McCauley's computations. The regression statistics reported in Table III indicate no correlation between the observed x values and those calculated using McCauley's solution to Nikiforov's inequalities. This failure can be ascribed to the inability to choose the correct x value in the range of calculated values determined from the inequalities.

Assuming the accuracy of Eqs. [1] and [2], the calculated x values (Table II) can be used in a rearrangement of the A–X or B–X expressions in Table I to calculate cell edge values. Figure 4 is a comparison of observed cell edges versus those calculated as just described. The observed cell edge was included in a regression against the calculated value for the full data and the same three subgroups previously described. The least squares equations obtained (Table III) account for 94.3% of the cell edge variation for the full data, 95.6% for $A^{3+}B^{4+}$, 87.9% for $A^{2+}B^{5+}$, and 94.3% for others.

A subset of data consisting of 32 oxyfluoride pyrochlores was considered separately to determine if anyone among three possible anion configurations would yield better calculated values of the cell edge as compared with the observed cell edges. The three anion configurations considered are (1) $A_2B_2(O_6F)$, O and F disordered over X and Y; (2) $A_2B_2(O_5F)O$, O and F disor-

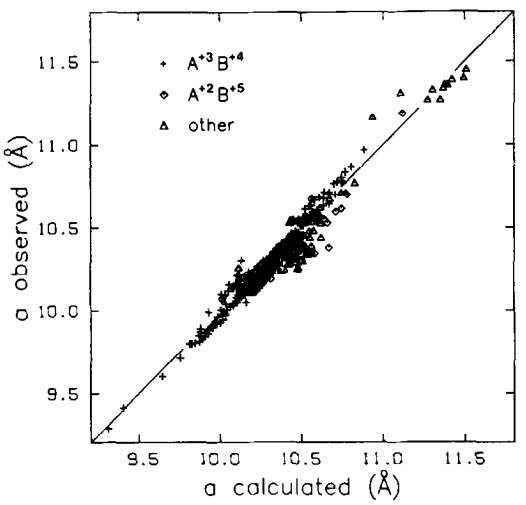

FIG. 4. Observed cell edges, a, are compared with those calculated for $A_2B_2X_6Y$ pyrochlores. The solid line is the one-to-one relationship.

dered over X, and O on Y; and (3) $A_2B_2X_6Y$, fully ordered with O on X and F on Y. The regression statistics for the calculated versus the observed cell edge for these three cases are not significantly different. Although electrostatic neutrality arguments and Madelung energy calculations (*10*) rank the fully ordered case as the most likely anion distribution, the cell edge does not appear to be sensitive enough to distinguish among the three anion configurations. In the oxysulfides the cell edge may be more sensitive to the anion distribution owing to the greater size difference between the sulfide and oxide bonds, however, a sufficient data base to test this hypothesis is lacking.

The calculated cell edge can be used to check the consistency of the reported data. If the observed cell edge is not within two standard deviations (0.129 Å) of the calculated cell edge, then the stoichiometry, cell edge measurement, or bond length predicting radii may be suspect. In this regard, the regression equations (Table III) suggest that for the three valence combinations distinguished, the $A^{2+}B^{5+}$ and other groups are not as well characterized as the $A^{3+}B^{4+}$ pyrochlores. This may be expected for the other groups, as their chemistries are in general more complicated (see Table II). Most reported stoichiometries are assumed to be the same as the molar proportions of the starting mixes, based on optical examination and X-ray diffraction patterns rather than examination by spectroscopic or electron microprobe techniques. If the residuals about the regression line are assumed to be distributed normally, then for the best data group, $A^{3+}B^{4+}$, 95% of the observed cell edges are within 1.96σ, or 0.098 Å, of the predicted values. Since the reported errors for most of the observed cell edges are in the third or fourth decimal place, inconsistencies in bond length predicting radii and/or reported stoichiometries are probably the main source of error.

Comparison of observed and calculated cell edges identifies some of the more frequent discrepancies, e.g., pyrochlores having Bi^{3+}, Na^{+}, and Pb^{2+} among the A cations. Shannon (*12*) has discussed some of the factors which affect the additivity of radii (i.e., variations in bond length), which include polyhedral distortion, partial occupancy of cation sites, covalence, and metallic character.

The empirical and the geometrical equations for predicting the cell edge are equally successful, as evidenced by the nearly equivalent coefficients of determination and standard deviations (Table III); however, the geometrical equations are firmly based on a knowledge of the pyrochlore structure and should be able to predict the cell edge without parameterization. The estimation of the x value as an intermediate step is also a distinct advantage. Although the geometrical equations themselves are non-empirical the mean bond lengths are estimated using empirical sets of ionic radii.

The interatomic distances that approximately limit the formation of $A_2B_2O_6Y$ pyrochlores are given in Fig. 5, which has the calculated x values plotted against the

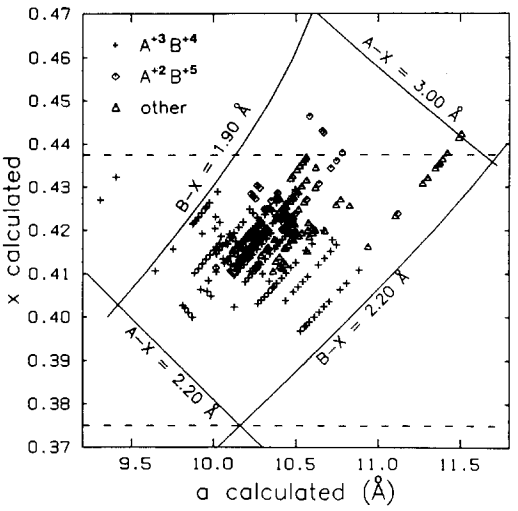

FIG. 5. Calculated X anion positional parameters and calculated cell edges display the approximate range of $A_2B_2X_6Y$ pyrochlore formation. The solid lines are the values of the cubic and octahedral bond lengths which provide an approximate enclosure. The horizontal dash lines, $x = 0.3750$ and $x = 0.4375$, bound the range of x for which the minimum anion separation is the largest (see Fig. 2). Note that the octahedral polyhedron is regular for $x = 0.4375$ and the cubic polyhedron is regular for $x = 0.3750$.

calculated cell edges. The largest values of x appear to be bound by the shortening of the anion–anion separation, whereas the smallest values thus far seem to be restricted only by the particular A–X and B–X distances. All of the x values occupy the range for maximum anion separation; and by comparison with Fig. 2, the calculated values of the minimum anion separation are in the range 2.40–3.05 Å. The maximum cell size is limited by the absolute size of the X anion. In contrast, the minimum cell size is significantly reduced by those pyrochlores which form at high pressure. The two smallest cell edge values, which fall well outside the arbitrary B–X bounds, are for the high pressure (120 kbar) pyrochlores $Sc_2Si_2O_7$ and $In_2Si_2O_7$. The first row of points closest to the B–$X = 1.90$ Å curve are also for high pressure (65 kbar) pyrochlores, $A_2Ge_2O_7$ where A = Sc, Y, In, Gd, Dy–Lu, Tl.

Lastly, to facilitate the rapid estimation of the structural parameters for $A_2B_2O_6Y$ pyrochlores without the need to make computations, a structure field map (Fig. 6) has been contoured for reasonable values of the cell edge, the anion positional parameter x, and the ratio of the mean cubic and octahedral cation radii rA/rB.

The equations developed and applied above provide a description of the geometry of a cubic pyrochlore if it were to form; however, the appropriate bond lengths and bond length ratio alone are not necessarily sufficient criteria for the formation of a cubic pyrochlore. Other structures, such as the weberite and thortveitite types, and distortions from cubic symmetry are both possible. The polymorphism and distortions depend on the synthesis conditions and the detailed nature of the chemical bonding.

Conclusions

From a knowledge of the geometry of a cubic $A_2B_2X_6Y$ pyrochlore, the X anion positional parameter can be expressed as a function of the ratio of the mean cubic to octahedral bond lengths. The cell edge and positional parameter can be calculated given a consistent means of predicting the average cubic and octahedral bond lengths, here obtained by the additivity of effective ionic radii. This cell edge calculation is a preferred alternative to the completely empirical equations relating cell edge to mean cubic and octahedral radii. In a regression analysis of observed versus calculated cell edge the standard deviation from the regression line is an order of magnitude larger than the reported errors in the cell edges, indicating that at least 20% of the pyrochlores examined may have inconsistencies in their stoichiometry, cell edge measurement, or bond length predicting radii. Partial atomic or oxidation-state disorder over

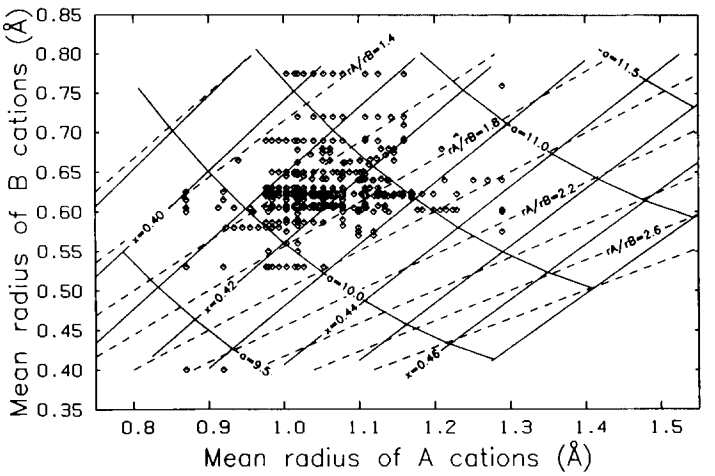

FIG. 6. Structure field map of octahedral cation radius versus cubic cation radius contoured with values of the cell edge, a, X anion positional parameter, x, and radius ratio, rA/rB. The ionic radii of Shannon (*12*) are used, and both the X and Y anions are here assumed to be divalent oxygen ($r(O^{2-})$ = 1.38 Å for four coordination).

A and B may also contribute to the discrepancy in some cases. The diagrams and equations presented also allow for the prediction of the cell edge and anion coordinate for hypothetical or partially studied pyrochlores.

A similar statistical study of the "inverse" pyrochlores could be made using geometric equations developed for $\square B_2X_6M$; however, a large data base is lacking. In addition, the M atom in many "inverse" pyrochlores is displaced from the 8*a* positions into the 32*e* positions, for which there is another variable parameter. A similar study of the defect pyrochlores would not be possible, unless the effective size of the vacant A sites could be accurately estimated.

Acknowledgments

The manuscript benefited from reviews by Kathleen Affholter and Dr. R. C. Ewing. The author is grateful for financial support from a Cunningham Fellowship and National Science Foundation Grant EAR-8218743 awarded to G. V. Gibbs. All the computations reported in this study were made with the program SAS (SAS Institute Inc., SAS Circle, P.O. Box 8000, Cary, N.C. 27511) using the VPI&SU Computer Center facilities.

References

1. J. B. GOODENOUGH AND R. N. CASTELLANO, *J. Solid State Chem.* **44,** 108 (1982).
2. D. BERNARD, J. PANNETIER, AND J. LUCAS. *Ferroelectrics* **21,** 429 (1978).
3. L. SODERHOLM, C. V. STAGER, AND J. E. GREEDAN, *J. Solid State Chem.* **43,** 175 (1982).
4. N. CHEVALIER, F. GAUME-MAHN, J. JANIN, AND J. ORIOL, *C.R. Seances Acad. Sci., Ser. C* **255,** 1096 (1962).
5. J. GRINS, *Chem. Commun. (Stockholm)* **8,** 1 (1980).
6. A. E. RINGWOOD, S. E. KESSON, N. G. WARE, W. HIBBERSON, AND A. MAJOR, *Nature (London)* **278,** 219 (1979).
7. M. FLEISCHER, "Glossary of Mineral Species 1983," Mineralogical Record, Inc., Tucson (1983).
8. M. A. SUBRAMANIAN, G. ARAVAMUDAN, AND G. V. SUBBA RAO, *Progr. Solid State Chem.* **15,** 55 (1983).
9. YU. PYATENKO, *Sov. Phys. Crystallogr.* **4,** 184 (1960).
10. W. W. BARKER, P. S. WHITE, AND O. KNOP, *Canad. J. Chem.* **54,** 2316 (1976).
11. H. R. HOEKSTRA AND S. SIEGEL, *Inorg. Chem.* **7,** 141 (1968).

12. R. D. SHANNON, *Acta Crystallogr. Sect. A* **32,** 751 (1976).
13. L. G. NIKIFOROV, *Sov. Phys. Crystallogr.* **17,** 347 (1972).
14. R. A. MCCAULEY, *J. Appl. Phys.* **51,** 290 (1980).
15. W. W. BARKER, J. GRAHAM, O. KNOP, AND F. BRISSE, *in* "The Chemistry of Extended Defects in Non-Metallic Solids" (L. Eyring and M. O'Keeffe, Eds.), p. 198, North-Holland, Amsterdam (1970).
16. R. C. EWING AND B. C. CHAKOUMAKOS, *in* "Short Course in Granitic Pegmatites in Science and Industry" (P. Černý, Ed.), p. 239, Mineral. Assoc. Canada, Toronto (1982).
17. J. PANNETIER, *J. Phys. Chem. Solids* **34,** 583 (1973).
18. J. PANNETIER AND J. LUCAS, *Mater. Res. Bull.* **5,** 797 (1970).